Article

Toxicological Evaluations in Macrophages and Mice Acutely and Chronically Exposed to Halloysite Clay Nanotubes Functionalized with Polystyrene

Yanis Toledano-Magaña, Leticia Flores-Santos, Georgina Montes de Oca, Alfonso González-Montiel, Juan-Carlos García-Ramos, Conchi Mora, Noemí-Alejandra Saavedra-Ávila, Marco Gudiño-Zayas, Luisa-Carolina González-Ramírez, Juan P. Laclette, and Julio C. Carrero*

Read Online

ACCESS | Metrics & More | Article Recommendations | Supporting Information

ABSTRACT: Halloysite clay nanotubes (HNTs) have been proposed as highly biocompatible for several biomedical applications. Various polymers have been used to functionalize HNTs, but scarce information exists about polystyrene for this purpose. This work evaluated polystyrene-functionalized HNTs (FHNTs) by comparing its effects with non-FHNTs and innocuous talc powder on *in vitro* and *in vivo* models. Monocyte-derived human or murine macrophages and the RAW 264.7 cell line were treated with 0.01, 0.1, 1, and 100 μg mL^{-1} FHNTs, HNTs, or talc to evaluate the cytotoxic and cytokine response. Our results show that nanoclays did not cause cytotoxic damage to macrophages. Only the 100 μg mL^{-1} concentration induced slight proinflammatory cytokine production at short exposure, followed by an anti-inflammatory response that increases over time. CD1 mice treated with a single dose of 1, 2.5, or 5 mg Kg^{-1} of FHNTs or HNTs by oral and inhalation routes caused aluminum accumulation in the kidneys and lungs, without bodily signs of distress or histopathological changes in any treated mice, evaluated at 48 h and 30 days post-treatment. Nanoclay administration simultaneously by four different parenteral routes (20 mg Kg^{-1}) or the combination of administration routes (parenteral + oral or parenteral + inhalation; 25 mg Kg^{-1}) showed accumulation on the injection site and slight surrounding inflammation 30 days post-treatment. CD1 mice chronically exposed to HNTs or FHNTs in the bedding material (*ca* 1 mg) throughout the parental generation and two successive inbred generations for 8 months did not cause any inflammatory process or damage to the abdominal organs and the reproductive system of the mice of any of the generations, did not affect the number of newborn mice and their survival, and did not induce congenital malformations in the offspring. FHNTs showed a slightly less effect than HNTs in all experiments, suggesting that functionalization makes them less cytotoxic. Doses of up to 25 mg Kg^{-1} by different administration routes and permanent exposure to 1 mg of HNTs or FHNTs for 8 months seem safe for CD1 mice. Our *in vivo* and *in vitro* results indicate that nanoclays are highly biocompatible, supporting their possible safe use for future biomedical and general-purpose applications.

1. INTRODUCTION

Nanoclay property and application study is a research area that is rapidly growing due to their potential for biomedical applications.[1,2] Mainly, halloysite [Al$_2$Si$_2$O$_5$(OH)$_4 \cdot n$H$_2$O] has been extensively studied due to its structural features: porosity, tube lumen size, and particular inner/outer surface chemistry. The inner surface corresponds to aluminum oxides, while silica makes up the external sheets, which gives it advantages on the loading and controlled release of drugs and genes compared with other clays.[3] Halloysite nanotubes (HNTs) are viable and inexpensive nanoscale containers[4−8] enhancing the loading and controlled release of drugs and genes,[9,10] organosilanes,[11] or nitric oxide[12] and also functioning as biomimetic nano-reactors.[11,13] The HNT functionalization with polymeric materials such as polyethyleneimine, polycaprolactone, poly-

(*N*-isopropyl acrylamide), chitosan, gelatin elastomers, endo-dontic sealers, or adhesive resins[14] gives them other functions including antimicrobial activity,[15−19] antitumor activity,[20,21] brain disorder treatment,[22] wound-healing materials,[2] bone repairing,[9] tissue regeneration,[23,24] and as a filler for general-purpose materials.[6,20,25,26]

HNT toxicity has been evaluated on different *in vitro* models, including neoplastic cell lines,[27] fibroblasts,[28] human

intestinal Caco-2 cells,[29] human peripheral blood lymphocytes,[30] and red blood cells.[31] In all cases, HNTs are shown to be nontoxic or scarcely toxic under the tested conditions. In contrast, oral administration of HNTs for 30 days induces a fibrotic response in the lung and oxidative damage in the liver of mice.[32,33] An increase in the HNT surface enhanced pulmonary tissue inflammatory cytotoxicity in C57BL/6 JBomTac mice.[34] Functionalization of HNTs with trimethoxy-(propyl)silane and triethoxy(octyl)silane causes apoptosis in C6 rat glioblastoma cells.[35] Meanwhile, HNT attachment to Fe_3O_4 nanoparticles induces higher cytotoxicity than Fe_3O_4 nanoparticles on A-549 cell lines.[36] These examples show the potential toxicity of nanoclays *in vivo* and the substantial role of the surface functionalization on the toxic effect produced.

To our knowledge, polystyrene has been scarcely studied compared to other polymers to functionalize HNTs, although polystyrene is one of the most widely used polymers in food containers, food-contact applications, laboratory products, medical devices, cosmetics, pharmaceutics, and cleaning agents due to its inertness and high biocompatibility.[37] Therefore, this study assessed the *in vitro* and *in vivo* biocompatibility of nonfunctionalized HNTs and polystyrene-functionalized HNTs (FHNTs). The latter was described previously and entirely characterized by Flores-Santos.[25] For *in vitro* tests, we evaluated the effect of nanoclays on macrophages, considering that they are the main phagocytic cells in the body and leading players in the immunological response. HNTs or FHNTs were administered to macrophages derived from human and mouse monocytes and macrophages from the RAW 264.7 cell line to evaluate their effect on the viability and cytokine release. Furthermore, toxicity after acute, semiacute, and chronic exposure of CD1 mice throughout different administration routes was evaluated, including the second-generation offspring.

2. RESULTS AND DISCUSSION

2.1. Characterization of HNTs and FHNTs. Synthesis and characterization of FHNTs and HNTs used here are reported in the US Patent Application US 2008200601A1.[25] Briefly, HNTs were obtained by grinding and sieving natural halloysite; meanwhile, FHNTs were obtained by a surface treatment of HNTs with copolymer styrene as a functionalizing agent. HNT and FHNT physicochemical properties were quite similar (Table 1). Both samples show a hollow tubular

Table 1. Physicochemical Properties of HNTs and FHNTs

properties	units	HNTs	FHNTs
humidity	%	1.51	1.15
bulk density	g mL−1	0.12	0.12
ashes	%	85.39	83.34
conductivity	μS	231	192
length/diameter	dimensionless	9	9
average diameter	nm	76	82

structure, as determined by transmission electron microscopy (TEM) with average diameters of 76 and 82 nm for HNTs and FHNTs, respectively (Figure 1).

2.2. Cytotoxicity Assays. The nanoclay-induced effects on human and murine macrophage viability and cell death pathways (apoptosis and necrosis) at concentrations of 0.01, 0.1, 1, 10, and 100 μg mL^{-1} were determined by flow cytometry using Annexin V/propidium iodide. Talc powder
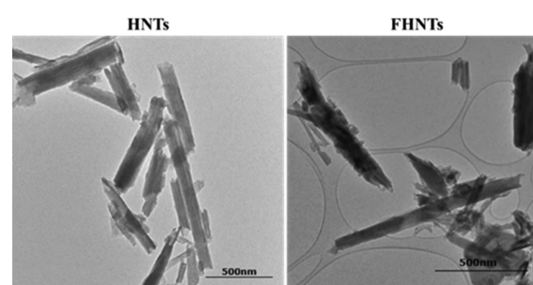

Figure 1. TEM images of the halloysite nanotube powder used in this work. Both HNTs and FHNTs show a typical hollow tubular shape with diameters down to 100 nm on average.

was used as a negative control for comparative purposes.[38] Macrophage cultures treated with FHNTs, HNTs, and talc showed minimal viability decrease (less than 5%) independent of exposure time with concentrations within the range of 0.01–10 μg mL^{-1}. When evaluating at the concentration of 100 μg mL^{-1}, a time-dependent decrease in viability was observed, but it did not exceed 10% at the maximum exposure time of 60 h for RAW 264.7 and human peripheral blood monocytes (HMDM). The effect was slightly greater in mice bone marrow monocytes (MMDM) but did not exceed 15% at 60 h (Figure 2, upper panel). No differences were found in the viability of macrophages exposed to halloysites with respect to talc. Overall, the statistical analysis showed no significant differences between groups, independently of the macrophage source, exposure time, or studied material.

When the type of cell death induced by halloysite nanoclays was analyzed, it was found that murine macrophages exposed to 100 μg mL^{-1} HNTs or FHNTs, either the RAW 264.7 cell line or MMDM, exhibited higher levels of apoptosis (from 2-5%) than human macrophages HMDM (0.5–1.5%) (Figure 2, middle panel). Conversely, 2–12% of necrosis was found on human macrophages exposed to 100 μg mL^{-1} HNTs or FHNTs, whereas just 1 to 2% was observed on murine macrophages (Figure 2, lower panel). The mechanisms of the apoptosis triggered in these macrophages by the nanoclays remain unknown and warrant further study. Still, it could involve surface scavenger receptors and the activation of mitochondrial caspase 9, as described for multiwall nanotubes.[39]

The functionalization of HNTs with polystyrene (FHNTs) did not modify the cytotoxic effect on macrophages compared with that of HNTs. Considering the high amount of material employed to produce a small decrease in viability, these results suggest that none of the materials assessed herein were significantly toxic to macrophages. Our results are in agreement with those on HNT toxicity in macrophages of the RAW 264.7 cell line by Wu and co-workers.[31] They found that 100 μg mL^{-1} HNTs were incorporated around the cell nucleus without producing cytotoxic damage to macrophages. Besides, human peripheral blood lymphocytes incubated with a halloysite suspension did not show a significant deleterious effect,[40] and the effect in human pancreatic cells (Panc-1) was described as insignificant.[41] Likewise, when compared with other nanoclays, such as clinoptilolite or sepiolite, HNTs showed lower toxicity over macrophage cell cultures, causing only half of the cytotoxic effect observed with those other nanoclays.[42] The high cyto- and biocompatibility of HNTs have also been confirmed in freshwater unicellular organisms such as the protozoa *Paramecium caudatum* (a maximum safe
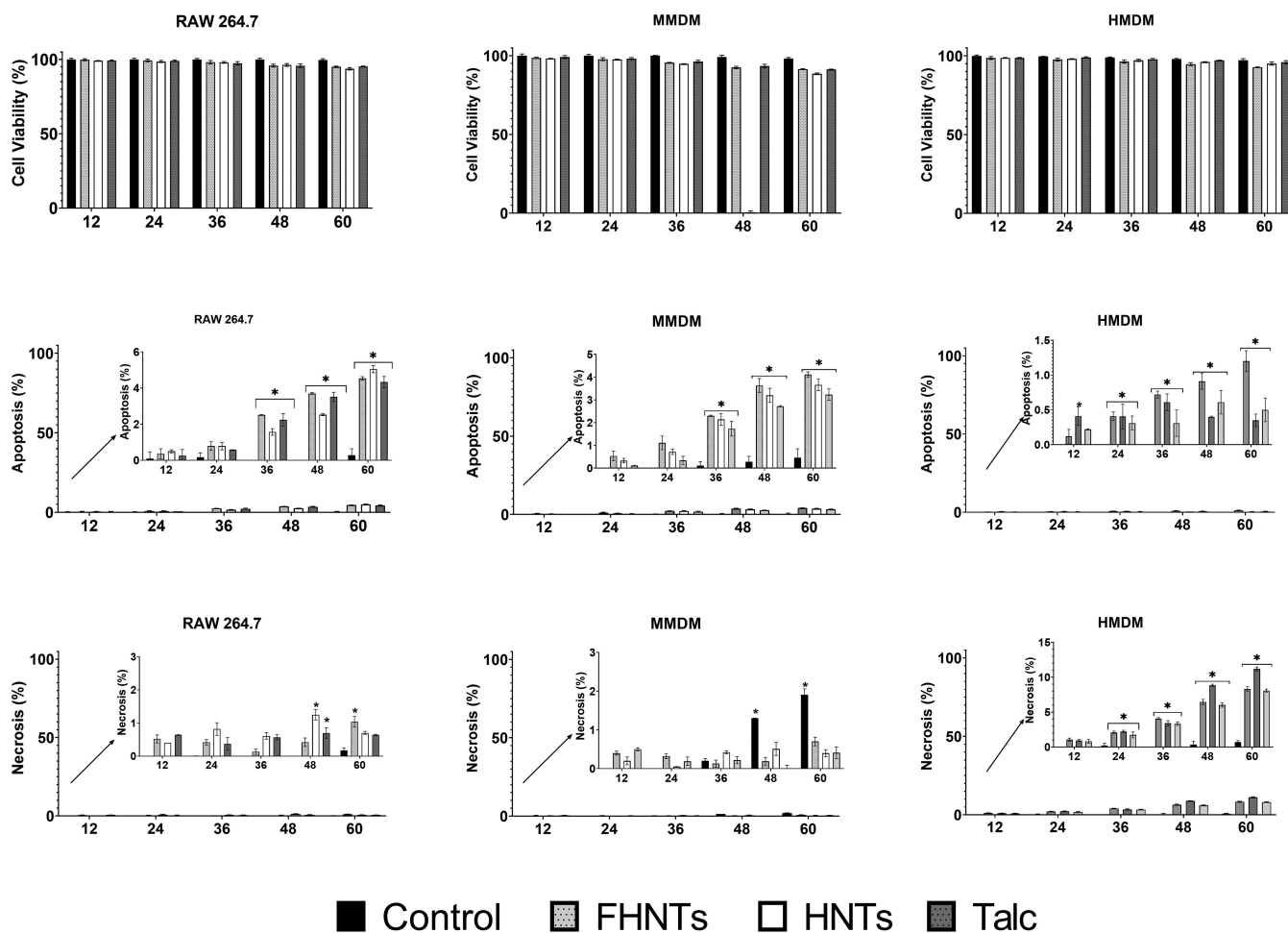
Figure 2. Macrophage viability and type of cell death induced by HNTs, FHNTs, and talc at 100 μg mL^{-1}. The RAW 264.7 cell line and macrophages from mice bone marrow monocytes and HMDMs were stained with Annexin V and propidium iodide to evaluate the viability, apoptosis, and necrosis. Evaluations at 12, 24, 36, 48, and 60 h are shown.

dose of 1 mg mL^{-1}) and multicellular organisms such as the nematode *Caenorhabditis elegans* (1 mg mL^{-1}) and the larvae of zebra fish (up to 10 mg mL^{-1}).[43−45] Our results show that HNTs and FHNTs with concentrations up to 100 μg mL^{-1} are safe for macrophages *in vitro*, independent of their source. This concentration of HNTs agrees with those previously reported as the maximum concentration at which the nanoclays do not kill Hela and MCF-7 cell lines (75 μg mL^{-1}).[27] In summary, our results and several others in the literature[15,43−47] agree regarding the low cytotoxicity of HNTs and FHNTs in *in vitro* studies.

2.3. Cytokine Production. Given that FHNTs could have many biomedical applications, we considered it essential to evaluate the ability of these nanoclays to activate proinflammatory responses in macrophages. Cytokines IFN-γ, IL-1α, IL-6, IL-8, IL-10, and IL-17 produced by HMDM and MMDM cultures exposed to 100 μg mL^{-1} HNTs, FHNTs, or talc were quantified. The RAW 264.7 cell line was excluded in this experimental section because of our interest in evaluating the inflammatory effects on primary cultures. Exposure of the HMDM and MMDM cultures to FHNTs did not induce the release of inflammatory cytokines IL-1α and IL-6 at any time assessed, remaining at baseline levels. Moreover, no expression of the proinflammatory cytokine INF-γ was detected. Only a slight increase in IL-8 levels over time was observed in MMDM cultures exposed to FHNTs compared to that with

talc but not in HMDM cultures. With this exception, the production of inflammatory cytokines promoted by FHNTs was lower than that produced by HNTs and talc, significantly much lower compared to the latter. Furthermore, the exposure of macrophages to either nanoclay induced the release of the regulatory cytokine IL-10, whose levels increased over time, as well as an increase in IL-7 levels but only at late times (Figure 3).

It is known that Th1 cytokine secretion is associated with a proinflammatory response, whereas Th2 cytokines counteract this Th1 response, reducing inflammation; meanwhile, IL-10 has a regulatory effect.[48] Herein, we found that macrophage cultures treated with FHNTs or HNTs do not exhibit a specific cytokine pattern. The low production of the proinflammatory cytokines IL-1α and IL-6, together with the absence of INFγ, is related to a low inflammatory potential. In contrast, it is well-known that the secretion of IL-8 favors the recruitment of immune cells, mainly neutrophils, together with a Th1-associated immune response.[49] In this sense, most biocompatible materials have been shown to induce the secretion of proinflammatory cytokines such as TNF-α, although its expression tends to decrease over time.[49] On the other hand, the induction of the regulatory cytokine IL-10 over time suggests a possible role in resolving any early inflammation. Thus, IL-10 secretion is related to the regulation of inflammatory processes and biocompatibility, contributing to
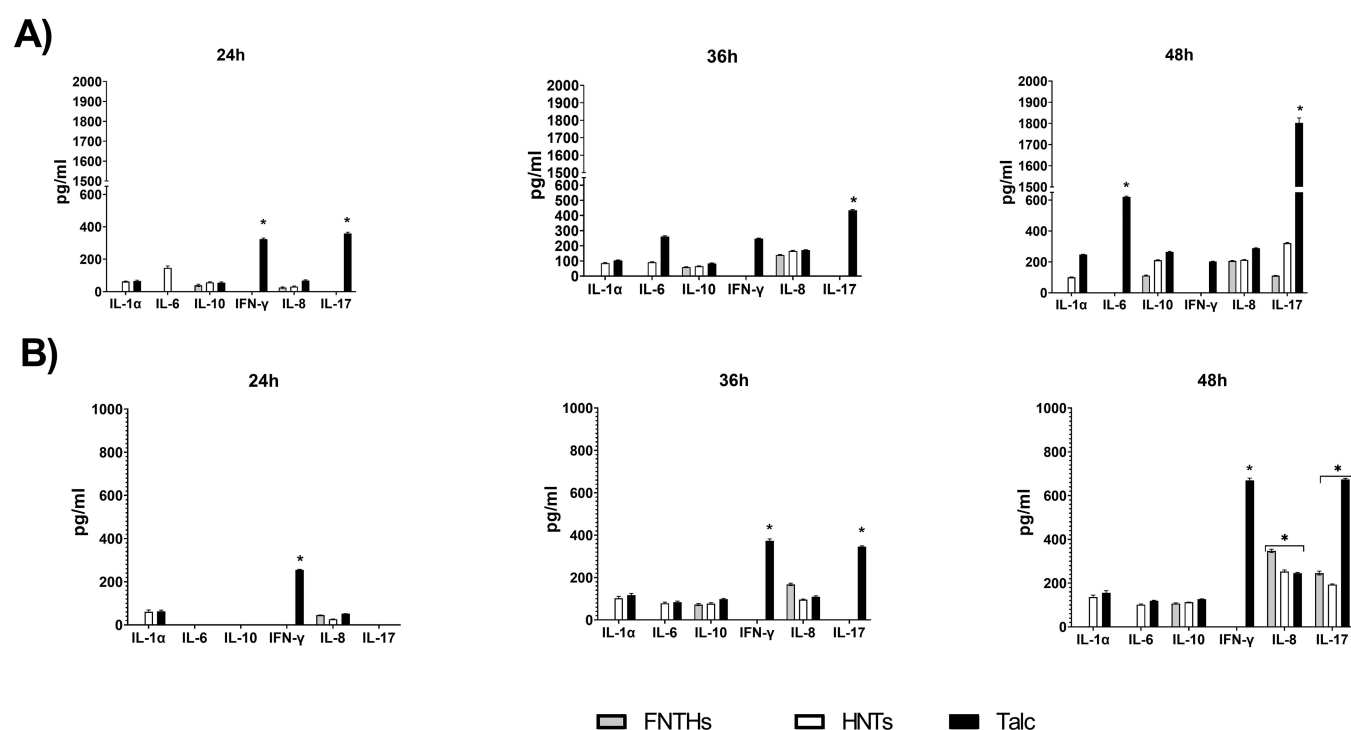
A)

B)

FNTHs   HNTs   Talc

Figure 3. Cytokine expression in macrophages exposed to halloysite nanoclays. Cytokines IFN-γ, IL-1α, IL-6, IL-8, IL-10, and IL-17 were quantified by flow cytometry in (A) HMDM cultures and (B) MMDM cultures after exposure to 100 μg mL^{-1} FHNTs, HNTs, or talc for 24, 36, and 48 h.

Table 2. Serological Values of Liver and Kidney Function Parameters in Mice Treated with Halloysite Nanoclays[a]

	units	reference	24 h			48 h		
			control	FHNTs	HNTs	control	FHNTs	HNTs
urea	mmol mL−1	8.87 ± 1.61	7.61 ± 1.13	5.1 ± 0.3	9.2 ± 0.7	8.5 ± 0.4	7.56 ± 0.4	8.21 ± 0.8
AST	U L−1	82.80 ± 39.85	79 ± 12.6	78 ± 4.6	70 ± 11.5	78 ± 9.6	78 ± 5.6	87 ± 7.3
ALT	U L−1	45.08 ± 16.11	35 ± 7.5	39 ± 2.3	30 ± 0.7	38 ± 6.8	40 ± 3.5	39 ± 3.7
creatinine	μM mL−1	10.73 ± 2.19	8.8 ± 1.2	9.1 ± 0.4	8.7 ± 0.1	8.8 ± 0.2	8.7 ± 0.2	9.1 ± 0.3
total protein	g L^{-1}	52.30 ± 11.13	54 ± 6.4	54 ± 3.6	45 ± 2.3	56 ± 5.2	54 ± 5.3	53 ± 4.7
total bilirubin	μM mL^{-1}	3.2 ± 1.2	2.37 ± 0.6	2.11 ± 0.3	2.23 ± 0.1	2.26 ± 0.1	2.3 ± 0.2	2.6 ± 0.2

[a]The mice were exposed to 5 mg Kg^{-1} HNTs or FHNTs, and the values of urea, alanine aminotransferase (ALT), aspartate aminotransferase (AST), creatinine, total protein, and total bilirubin were determined at 48 h and 30 days post-treatment. All parameters were within the range reported as standard by the Charles River Laboratories.

the inhibition or resolution of the inflammation associated with nanocomposites.[48] On the other hand, the release of IL-17 at later times could suggest that halloysite nanoclays, but mainly talc, have the potential to induce allergic responses as this cytokine has been related to anaphylaxis.[50] Overall, our results show that FHNTs and HNTs are poor inducers of proinflammatory cytokines in human and mouse macrophage cultures, which, in association with the induction of IL-10, suggests that halloysite nanoclays are well-tolerated by the macrophages, even better than talc.

2.4. Effect of Acute and Semiacute Exposure in Mice. To support and complement the results obtained *in vitro*, we evaluated the toxicity of halloysite nanoclays in experimental mice following acute and chronic exposure protocols. Here, we analyzed acute (24 h) and semiacute (30 days) effects of nanoclays on inbred CD1 mice, the preferred strain of mice for toxicity studies due to its variability between individuals.[51,52] HNT or FHNT administration (1, 2.5, or 5 mg Kg^{-1}) in CD1 mice by any of the assessed routes and their combinations (oral, respiratory, cutaneous, subcutaneous, intramuscular, and

intraperitoneal routes) did not induce any notable physiological change in the animals during the time the experiment lasted (30 days). Thus, the treated mice did not show apparent bodily signs of disease, such as bristly hair, diarrhea, vomiting, or infirmity (data not shown). Furthermore, the body temperature (36.5 ± 0.7 °C) and the weight of mice (approximately 35 g for females and 45 g for males) were within normal ranges throughout the 30 days.

Since renal and hepatobiliary systems are the most important routes for the elimination of foreign substances and particles, nanoclays could accumulate in these organs, causing tissue damage.[53] We determined the renal and hepatic functionality of mice treated with halloysite nanoclays by quantifying the serum hallmark parameters alanine and aspartate aminotransferases, creatinine, urea, bilirubin, and total proteins after 48 h and 30 days of exposure (Table 2). All the parameters in the sera of the mice treated with the nanoclays, regardless of whether they were functionalized or not, were within the range of reference values and did not show significant differences with respect to the values in
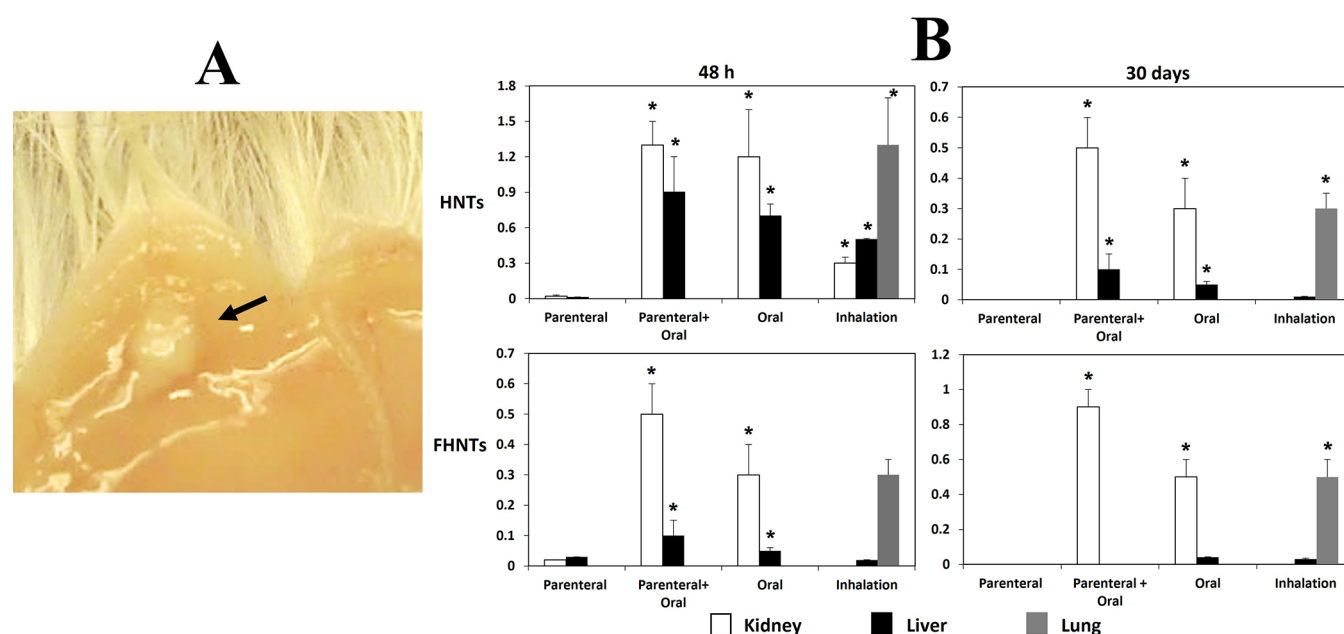
Figure 4. Accumulation of halloysite nanoclays in acute and semiacute treated mice. (A) The image shows the subcutaneous accumulation of FHNTs (arrow) at the injection site after 1 month of administering a single 5 mg Kg^{-1} dose. (B) Percentage of aluminum determined by atomic absorption in the kidney, liver, and lung of mice treated with HNTs or FHNTs at 48 h and 1 month after administration. The percentage was calculated according to the maximum expected amount of aluminum, as described in the experimental section.

untreated control mice (Table 2). A slight decrease in urea was observed in the sera of mice treated with FHNTs after 48 h of administration, but it was no longer observed after 1 month of exposure.

In general, the results of acute and semiacute exposure showed that the administration of HNTs or FHNTs by oral or respiratory routes, as well as their simultaneous administration by several parenteral routes (up to 20 mg Kg^{-1} nanoclays), did not induce any significant physiological change in the mice, suggesting that they were in good health and positioning nanoclays as a material with very highly biocompatibility. These results are in contrast to the previously reported loss of appetite, decreased body weight, and induction of inflammatory response in mice after the inhalation of HNTs.[54] Although the reason for these differences is unknown, it is likely to be related to the use of different strains of mice (CD1 vs Kunming) but above all to the exposure dose, because unlike our study where mice were exposed to a single dose of HNTs, the mice in the aforementioned study were exposed to HNTs for 14 days.[54]

2.5. HNT and FHNT Accumulation after Acute and Semiacute Exposure. The simultaneous administration of 5 mg Kg^{-1} nanoclay by each parenteral route (cutaneous, subcutaneous, intramuscular, and intraperitoneal; 20 mg Kg$^-$ nanoclay to each mouse) resulted in nanoclay clumps in the application site, observed 30 days post-exposure (Figure 4A; Supporting Information S1). The above observation means that most FHNT and HNT nanoparticles did not spread throughout the body, supporting their use for some biomedical applications.

The accumulation of HNTs and FHNTs on the kidney, liver, and lung of treated mice was evaluated by quantifying aluminum using atomic absorption spectroscopy. Results showed nanoclays in the liver, lung, and kidney of orally and respiratory treated mice but not in the organs of mice simultaneously administered with all the parenteral routes

(Figure 4B; Supporting Information Figure S1). A higher accumulation of HNTs than that of FHNTs was observed in mice at 48 h postexposure (Figure 4A), mainly identified in the kidney and liver of mice treated orally and lung of mice treated by inhalation with the 5 mg Kg^{-1} dose. On the other hand, at 30 days after exposure, less aluminum was detected in the liver, but the same amount remained in the kidney of orally and orally plus parenteral treated mice. In mice treated by inhalation, aluminum was detected in the lungs as expected, and the amount remained similar at 48 h and 1 month postexposure (Figure 4B).

In summary, the maximum aluminum accumulation in the HNTs group was observed in kidneys of orally treated and lungs of inhalation-treated mice at 48 h post-treatment with 1.5% of the maximum amount of aluminum expected, that is, 0.49 μg (Figure 4B, upper graphs). In contrast, the maximum accumulation of aluminum in the FHNT group was observed at 30 days post-treatment with 0.9% (0.294 μg Al) in the kidney of orally treated and 0.5% (0.163 μg Al) in the lung of inhalation-treated mice (Figure 4B, lower graphs). These values are close to the 0.28−0.76% absorption efficiency reported in subjects ingesting 3 mg Al/day (0.04 mg Al/kg/day) or 4.6 mg Al/day (0.07 mg Al/kg/day), a dose much lower than the regular intake of aluminum in food. The aluminum percentages reported here were calculated considering the possible maximum amount that each administration route could reach. These percentages of Al accumulation in HNT-treated mice can be considered negligible.

The results regarding aluminum accumulation in mice treated with FHNTs suggest that functionalization with polystyrene made the nanoclays more rapidly mobilized from the injection site to the target organs than HNTs, and therefore, they were excreted faster from the body. The higher persistence of HNTs than that of FHNTs inside the body could be due to its lower solubility, a physical feature of less biocompatible particles.[52,53] These results agree with different
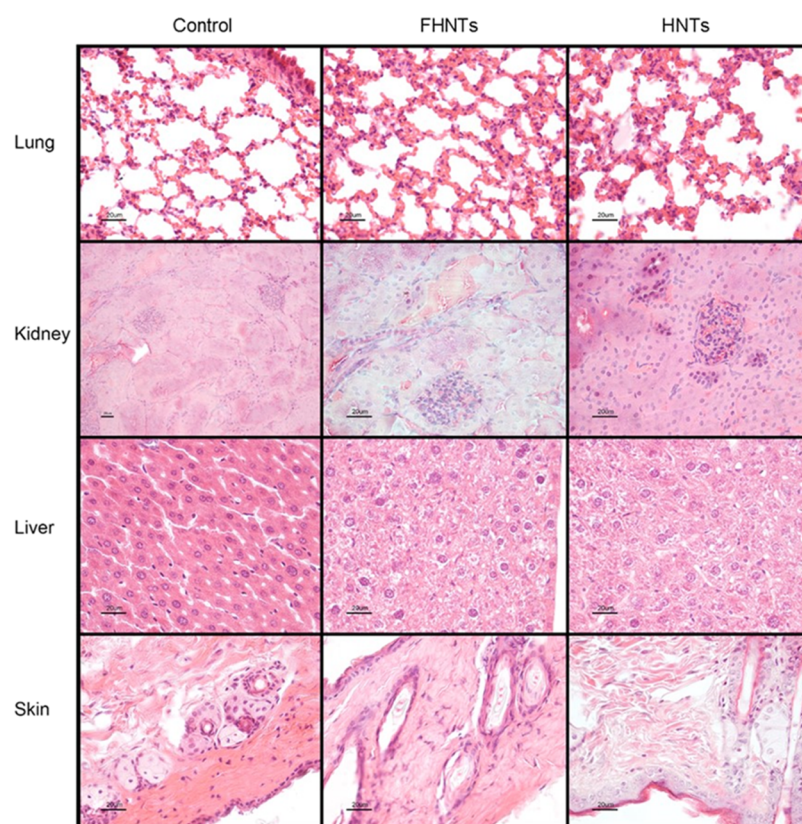
Figure 5. Photomicrographs showing hematoxylin–eosin staining of the lung, kidney, liver, and subcutaneous tissue of untreated mice (control group) and those treated with HNTs and FHNTs. No inflammatory infiltration or damaged tissue was observed. The samples were taken of F2 mice exposed to HNTs and FHNTs as the bed material. F2 mice were euthanized after the completion of 8 months of exposure to nanoclays.

studies dealing with the bioavailability and accumulation of aluminum after oral and inhalation exposure. These reports show that the Al concentration increases on target organs such as the lungs, liver, bone, and spleen after 8 days of a single gavage of 2.6 mg of Al but rapidly decreases after 3 days of Al source withdrawal. Absorbed aluminum is primarily excreted in the urine, with a small amount of absorbed aluminum excreted in the feces.[55] The administration routes assayed in the present study tried to emulate the general ways of nanoclay exposure and the toxicological accumulation response. Other administration routes such as intravenous administrations are highly recommended for particular uses such as drug delivery and merit further investigation. Still, acute exposure experiments described above confirm the biocompatibility of HNTs and FHNTs for doses up to 25 mg Kg^{-1}.

2.6. Chronic Exposure. To the best of our knowledge, no study has been reported evaluating the effect in several generations of animals exposed to FHNTs or HNTs. Chronic toxicity of nanoclays followed up through three generations (P, F1, and F2) was explored by exposing mice to HNTs or FHNTs (3 cm^3) into the bed material for 8 months. As the mice are permanently exposed, it is expected that the nanoclays will be ingested and aspirated and will adhere to the skin and hair of the animals throughout the 8 months. Even the eye, ear, and genital mucosa could be exposed to nanoclays. Even mating and parturition occurred in the presence of the nanoclays. Results showed no signs of illness for P or any member of F1 and F2 generations, including no changes in the body weight (Supporting Information Figure S2). Progeny numbers and survival of newborn mice were comparable to the untreated controls, and no congenital malformations were observed in three inbred generations.

The histological analysis of the liver, kidneys, lungs, spleen, heart, and reproductive and gastrointestinal systems after 8 months of permanent exposure to *ca.* 1 mg of nanoclay showed the absence of inflammatory processes and tissue damage in all animals of the three generations treated with HNTs or FHNTs (Figure 5). Our results agree with those reported by Wang and co-workers, who observed that a repeated dose of 5 mg Kg^{-1} body weight for 1 month did not cause liver or lung damage.[32] However, higher doses such as 50 mg Kg^{-1} produce oxidative damage and fibrotic response in the lungs, suggesting that HNTs can be toxic when the animals are overexposed to very high doses.[32,33,56] However, they are doses to which a human could hardly be exposed regularly.

Overall, our results demonstrate that permanent exposure of mice to halloysite nanoclays does not cause inflammation or detectable damage in parental or offspring mice and that polystyrene functionalization does not affect their high degree of biocompatibility. This innocuousness of nanoclays to prolonged exposures to low doses could be associated with their low proinflammatory potential and the rapid mobilization of the nanoparticles toward organs of excretion such as the kidney and gastrointestinal tract. In contrast, exposure to engineered TiO$_2$ nanoparticles and black carbon particles affects male reproductive function after fetal and adulthood exposure, including maternal gestational exposure to titanium dioxide nanoparticles by the subcutaneous injection, intranasal instillation, or intravenous route.[57−61]

In summary, concentrations of up to 100 μg mL^{-1} of FHNTs confirm their high cytocompatibility with human and murine macrophages. Besides, their high biocompatibility with CD1 mice after acute, semiacute, chronic, and generational effects was documented with doses up to 25 mg Kg^{-1} for the former and through permanent exposure to *ca.* 1 mg of nanoclay for 8 months for the latter. The remarkable cyto-/ biocompatibility of FHNTs could enhance the therapeutical and diagnostic properties of polystyrene−FHNTs previously described.

3. CONCLUSIONS

The use of nanomaterials for biomedical applications continues to be limited by toxicity issues. This work evaluated the cyto- and biocompatibility of HNTs and FHNTs on *in vitro* and *in vivo* models. Our results show that HNTs and FHNTs did not substantially affect the viability of human and mice macrophages at concentrations as high as 100 μg mL^{-1}. At this concentration, FHNT induces the release of some proinflammatory cytokines in these cells, followed by the consequent production of anti-inflammatory cytokines, probably as physiological feedback for controlling inflammation. The cytokines levels induced by FHNTs were consistently lower than that of HNTs and, in turn, much quieter than those caused by talc, considered innocuous.

No adverse effects were determined on mice treated by different administration routes, and no signs of illness were observed, neither acute nor chronically exposed mice. We found low accumulation of the nanoclay in the target organs kidney, lungs, and liver after 24 h and 30 days of exposure. Additionally, no modifications on the liver and kidney functionality serum biomarkers confirms their high biocompatibility with CD1 mice with doses of up to 25 mg Kg^{-1} administered by several parenteral routes simultaneously. Furthermore, permanent exposure to *ca.* 1 mg of nanoclay for 8 months for parents and pups did not evidence damage on the three generations studied. Although both nanoclays exhibited high biocompatibility, FHNTs resulted in a slightly better disposal, suggesting that this modification can even improve its safety use in humans. In summary, all results reported here support the notion of polystyrene−halloysite nanotubes as a highly biocompatible material, supporting their use for future biomedical and general-purpose applications.

4. MATERIALS AND METHODS

4.1. Nanoclays and Stock Solutions. Styrene-functionalized nanoclays (FHNTs) and nonfunctionalized nanoclays (HNTs) were provided by Centro de Investigación y Desarrrollo Tecnológico S.A de C.V, Lerma, Edo. De México. Homogeneous stock suspensions of each nanoclay were prepared in a phosphate-buffered saline (PBS) solution at 50 mg mL^{-1} by sonication. For cutaneous applications, nanoclays were mixed in Vaseline with 1, 2.5, and 5 mg in 500 μL.

4.2. Macrophage Culture and Cytotoxicity Assays. Cytotoxicity was systematically evaluated on human monocyte-derived macrophages (HMDM) and mouse bone marrow-derived macrophages (MMDM). Besides, macrophages from the RAW 264.7 cell line were used for comparative purposes (ATCC Cell Biology Collection; Promochem LGC, Molsheim, France). Macrophages were cultured in an RPMI 1640 medium supplemented with 10% fetal bovine serum (Bio Whittaker), 500 μg mL^{-1} gentamicin (Biosera), and 1% 2-

mercaptoethanol (GIBCO, Invitrogen) at 37 °C under a 5% carbon dioxide humidified atmosphere.

Human monocytes were purified from pooled blood samples of 10 healthy donors (Hospital Arnau de Vilanova, Lleida, Spain) by Ficoll-Paque PLUS gradients (GE Healthcare, Sweden). Monocytes were incubated for 2 h in the supplemented RPMI 1640 medium at 1×10^5 cells mL^{-1}, and washings discarded the nonadherent cells with the RPMI medium. Adherent cells were cultured for 6 days at 37 °C under 5% CO_2 with changes of RPMI culture media every 48 h. HMDM were identified under a microscope and by flow cytometry.

MMDM were obtained from 4 weeks old CD1 mice. Briefly, the femur and shinbones were extracted and put in absolute ethanol for 3 min; after that, they were washed with supplemented RPMI 1640 culture media. Bone marrow cells were manually removed from the bones and collected by centrifugation. Erythrocytes were lysed with water and 10× PBS; meanwhile, the white cells were washed with PBS and resuspended in the fresh culture medium. White cells were cultured in Petri dishes with 10 mL of RPMI 1640 culture medium, changing the culture medium every 48 h for 5 days to support the differentiation of monocytes into macrophages. MMDM were identified under a microscope and by flow cytometry.

The RAW 264.7 cell line was acquired from the ATCC and cultured in Petri dishes with the supplemented RPMI 1640 culture medium described above for HMDM.

For each experiment, 1×10^5 macrophages in 100 μL of the supplemented RPMI 1640 medium were placed in 96-well plates. FHNTs or HNTs were added at final concentrations of 0.01, 0.1, 1, 10, or 100 μg mL^{-1} per individual well. Control cultures were macrophages exposed to 0.01−100 μg mL^{-1} of talc, run in parallel with the experimental groups. Cells were incubated at 37 °C under 5% CO_2. Apoptosis/necrosis induced by FHNTs, HNTs, and talc were determined with Annexin V and propidium iodide (Annexin V-FITC Apoptosis Detection kit I, BD Pharmingen) at 12, 24, 36, and 48 h of exposure by flow cytometry according to the manufacturer's protocol. Three independent experiments were performed in triplicate for each agent assayed.

4.3. Determination of Th1 and Th2 Cytokines. Production of IFN-γ, IL-1α, IL-6, IL-8, IL-10, and IL-17 cytokines was measured in the supernatants of macrophage cell cultures exposed to 100 μg mL^{-1} FHNTs, HNTs, or talc for 24, 36, and 48 h. Quantification of the mentioned cytokines was performed by flow cytometry using the mouse and human Th1/Th2 10 plex FlowCytomix kit (eBioscience) according to the supplier's instructions.

4.4. Acute and Semiacute Toxicity Assay. Four weeks old CD1 mice were maintained under sterile conditions with food and water *ad libitum*. The use of animals in this project was authorized by the Internal Committee for the Care and Use of Laboratory Animals (CICUAL), UNAM, registered with ID 246. Mice were randomly divided into two groups, one for acute treatment and the other for semiacute exposure; in turn, the groups were subdivided for separate FHNT and HNT treatments. Considering the higher volume suggested for the parenteral administration of substances to laboratory animals (0.1 mL)[62] and the stock solution concentration (50 mg mL^{-1}), the maximum dose employed for acute and semiacute toxicity assays was 5 mg Kg^{-1}.

For acute treatments, male mice were given a unique dose of 1, 2.5, or 5 mg Kg^{-1} of FHNTs or HNTs by one of the following routes: (i) respiratory, using a powder dispersion chamber where each mouse, one by one, was kept for 5 min until it breathed in the indicated amount of the nanoclay (previously, we determined that 5 min within the chamber is enough time for recovering almost nothing of the nanoclay powder, suggesting that the mouse breathed it in); (ii) oral, using a neonatal feeding tube for the direct administration to the stomach; (iii) parenteral, by injecting a maximal volume of 100 μL of the agent simultaneously by cutaneous, subcutaneous, intramuscular, and intraperitoneal routes on each animal; and (iv) a combined administration scheme, parenteral routes (as in iii) in addition to oral administration (as in ii) on each animal. Groups of 15 mice were used for each treatment, of which three mice (triplicates) were euthanized at 1, 2, 3, 7, and 30 days after administration using CO$_2$. Additionally, an untreated five-mice group was used as the control and euthanized at day 30. Blood samples were collected for serological analysis. Besides, the application site tissue was dissected for histopathological examination. Systemic target organs such as kidneys, livers, and lungs were excised and processed to determine the tissue accumulation of nanoclays by aluminum quantification (see below). Mice body temperature and weight were determined every day throughout the experiment.

4.5. Chronic Exposure through Generations.
For chronic exposure, mice couples were placed in individual cages and allowed to reproduce for two generations. The generational effect of permanent exposure to the nanoclays was evaluated starting with four pairs of 4 weeks old CD1 mice per nanoclay. Mice were kept in sterile conditions with food and water *ad libitum* in cages containing 3 cm^3 of FHNTs or HNTs in the bed material. The bed material was replaced every 72 h for 8 months. Thus, the parent mice (P) and offspring (F1 and F2 generations) were constantly exposed to the nanoclays during feeding, mating, and new litters born. Mice body temperature and weight were determined once a week throughout the whole experiment.

Similarly, the number of live pups was recorded, along with the general condition and behavior of mice. After 8 months of the initial mating, mice were euthanized with CO$_2$. Histopathology studies were performed in organs from the couples of parents and 10 mice of each F1 and F2 generation (5 female and 5 male mice). Analysis of the stained tissue sections from the liver, kidney, lung, spleen, heart, and reproductive and gastrointestinal systems was performed. Animals without nanoclays in the bed material with the same experimental scheme were used as the control.

4.6. Nanoclay Accumulation in the Liver, Kidney, and Lung.
The bioaccumulation of nanoclays beyond the injection site in exposed mice was determined on each target organ such as the liver, kidney, and lung by quantifying aluminum by atomic absorption spectroscopy. The maximum expected aluminum content in mice was estimated considering the halloysite empirical formula Al$_2$Si$_2$O$_5$(OH)$_4\cdot$4H$_2$O with a molecular weight of 258 g mol^{-1}. 2 equiv of aluminum in the minimal formula represent 16.35% in each nanoclay sample. Aluminum quantification was performed only in the mice that received the highest amount of each nanoclay considering the amount of total nanoclay applied to different experimental groups: respiratory and oral, 5 mg Kg^{-1}; parenteral, 20 mg Kg^{-1} (5 mg Kg^{-1} for each administration

route: cutaneous, subcutaneous, intramuscular, and intraperitoneal); and combined oral plus parenteral scheme, 25 mg Kg^{-1}. Considering that the higher dose administered for mice by oral and respiratory routes is 5 mg Kg^{-1} in weight and taking an average mice weight of 40 g, we can expect the maximum quantity of aluminum in a mouse of these groups to be around 32.7 μg. In the combined scheme (treatment IV) case, the maximum expected aluminum quantity is 163.5 μg.

4.7. Liver and Kidney Function Tests.
Serological analyses of blood samples from mice at 24 h and 1 month postadministration (representing acute and semiacute exposure to the nanomaterials) were used to evaluate the liver and kidney function. Biochemical parameters such as aspartate aminotransferase, alanine aminotransferase, urea, creatinine, bilirubin, and total proteins were determined using standard methods of a clinical analysis laboratory for small species.

4.8. Statistical Analysis.
Data from viability assays were analyzed using a two-way ANOVA ($p < 0.05$) and Tuckey's *post hoc* test ($p < 0.05$).

4.9. Photomicrography.
Images were acquired using the Nikon MICROPHOT-FXA microscope attached to a Nikon digital camera (DXM1200F) and a computer with Nikon ACT-1 software. The objectives used were 20× and 40×.

■ ASSOCIATED CONTENT

Ⓢ Supporting Information
The Supporting Information is available free of charge at https://pubs.acs.org/doi/10.1021/acsomega.1c04367.

> Local effects of HNTs in CD1 mice exposed by different routes and weight variations of CD1 mice exposed to HNTs for 8 months (PDF)

■ AUTHOR INFORMATION

Corresponding Author
Julio C. Carrero — *Departamento de Inmunología, Instituto de Investigaciones Biomédicas, Universidad Nacional Autónoma de México, Cd. Universitaria, Ciudad de México 04510, México;* ◉ orcid.org/0000-0003-1055-5774; Phone: +525 56229220; Email: carrero@unam.mx

Authors
Yanis Toledano-Magaña — *Escuela de Ciencias de la Salud, Universidad Autónoma de Baja California, Ensenada, Baja California 22890, México;* ◉ orcid.org/0000-0002-2595-7939

Leticia Flores-Santos — *AddiCo, Ciudad de México 52764, México*

Georgina Montes de Oca — *CIATEQ Centro de Tecnología Avanzada, Lerma Edo de México 52004, México*

Alfonso González-Montiel — *AddiCo, Ciudad de México 52764, México*

Juan-Carlos García-Ramos — *Escuela de Ciencias de la Salud, Universidad Autónoma de Baja California, Ensenada, Baja California 22890, México;* ◉ orcid.org/0000-0001-9861-2467

Conchi Mora — *Immunology Unit, Department of Experimental Medicine, Faculty of Medicine, University of Lleida, Lleida 25002, Spain; Institut de Recerca Biomèdica Lleida (IRB-Lleida), Lleida 25002, Spain*

Noemí-Alejandra Saavedra-Ávila — *Department of Microbiology and Immunology, Albert Einstein College of Medicine, Bronx, New York 10461, United States*

Marco Gudiño-Zayas — *Laboratorio de Bioinformática, Unidad de Investigación en Medicina Experimental, Facultad de Medicina, UNAM, Ciudad de México 06720, México*

Luisa-Carolina González-Ramírez — *Grupo de Investigación "Análisis de Muestras Biológicas y Forenses", Carrera Laboratorio Clínico, Facultad de Ciencias de la Salud, Universidad Nacional de Chimborazo, Riobamba 0601003, Ecuador*

Juan P. Laclette — *Departamento de Inmunología, Instituto de Investigaciones Biomédicas, Universidad Nacional Autónoma de México, Cd. Universitaria, Ciudad de México 04510, México*

Complete contact information is available at:
https://pubs.acs.org/10.1021/acsomega.1c04367

Author Contributions

Conceptualization, Y.T.-M., L.F.-S., A.G.-M., and G.M.deO.; data curation, Y.T-M., J.C.G.-R., N.-A.S.-A., and J.C.C.; formal analysis, Y.T.-M., J.C.G.-R., N.-A.S.-A., L.-C.G.-R., J.P.L., and J.C.C.; funding acquisition, Y.T.-M., L.F.-S., A.G.-M. J.C.G.-R, C.M., and J.C.C; investigation, Y.T.-M., J.C.G.-R., G.M.deO., and M.G.Z.; methodology, Y.T.-M., C.M., N.A.S.-A., J.P.L., and J.C.C.; project administration, Y.T.-M., L.F.-S., A.G.-M., G.M.deO., J.C.G.-R., C.M., and J.C.C.; resources, L.F.-S., A.G.-M., G.M.deO., J.C.G.-R., C.M., J.P.L., and J.C.C.; supervision, L.F.-S., A.G.-M., C.M., J.P.L., and J.C.C.; validation, Y.T.-M., J.C.G.-R., and N.A.S.-A.; visualization, Y.T.-M., J.C.G.-R., N.A.S.-A.; M.G.-Z., and L.C.G.-R.; writing—original draft, Y.T.-M. and J.C.G.-R.; and writing—review and editing, all authors contributed. All authors have read and agreed to the published version of the manuscript.

Notes

The authors declare no competing financial interest.

■ REFERENCES

(1) Beshchasna, N.; Saqib, M.; Kraskiewicz, H.; Wasyluk, Ł.; Kuzmin, O.; Duta, O. C.; Ficai, D.; Ghizdavet, Z.; Marin, A.; Ficai, A.; Sun, Z.; Pichugin, V. F.; Opitz, J.; Andronescu, E. Recent Advances in Manufacturing Innovative Stents. *Pharmaceutics* 2020, 12, 349.

(2) Villalba-Rodríguez, A. M.; Martínez-González, S.; Sosa-Hernández, J. E.; Parra-Saldívar, R.; Bilal, M.; Iqbal, H. M. N. Nanoclay/Polymer-Based Hydrogels and Enzyme-Loaded Nanostructures for Wound Healing Applications. *Gels* 2021, 7, 59.

(3) Abdullayev, E.; Lvov, Y. Halloysite for Controllable Loading and Release. *Developments in Clay Science*; Elsevier Ltd., 2016; Vol. 7, pp 554−605.

(4) Price, R.; Gaber, B. P.; Lvov, Y. R. In-Vitro Release Characteristics of Tetracycline HCl, Khellin and Nicotinamide Adenine Dineculeotide from Halloysite; a Cylindrical Mineral. *J. Microencapsulation* 2001, 18, 713−722.

(5) Kelly, H. M.; Deasy, P. B.; Ziaka, E.; Claffey, N. Formulation and Preliminary in Vivo Dog Studies of a Novel Drug Delivery System for the Treatment of Periodontitis. *Int. J. Pharm.* 2004, 274, 167−83.

(6) Lvov, Y.; Wang, W.; Zhang, L.; Fakhrullin, R. Halloysite Clay Nanotubes for Loading and Sustained Release of Functional Compounds. *Adv. Mater.* 2016, 28, 1227−1250.

(7) Yendluri, R.; Lvov, Y.; de Villiers, M. M.; Naumenko, E.; Tarasova, E.; Fakhrullin, R. Paclitaxel Encapsulated in Halloysite Clay Nanotubes for Intestinal and Intracellular Delivery. *J. Pharm. Sci.* 2017, 106, 3131−3139.

(8) Santos, A. C.; Ferreira, C.; Veiga, F.; Ribeiro, A. J.; Panchal, A.; Lvov, Y.; Agarwal, A. Halloysite Clay Nanotubes for Life Sciences Applications: From Drug Encapsulation to Bioscaffold. *Adv. Colloid Interface Sci.* 2018, 257, 58−70.

(9) Satish, S.; Tharmavaram, M.; Rawtani, D. Halloysite Nanotubes as a Nature's Boon for Biomedical Applications. *Nanobiomedicine* 2019, 6, 184954351986362.

(10) Guryanov, I.; Naumenko, E.; Akhatova, F.; Lazzara, G.; Cavallaro, G.; Nigamatzyanova, L.; Fakhrullin, R. Selective Cytotoxic Activity of Prodigiosin@halloysite Nanoformulation. *Front. Bioeng. Biotechnol.* 2020, 8, 424.

(11) Yuan, P.; Tan, D.; Annabi-Bergaya, F. Properties and Applications of Halloysite Nanotubes: Recent Research Advances and Future Prospects. *Appl. Clay Sci.* 2015, 112-113, 75−93.

(12) Ghalei, S.; Hopkins, S.; Douglass, M.; Garren, M.; Mondal, A.; Handa, H. Nitric Oxide Releasing Halloysite Nanotubes for Biomedical Applications. *J. Colloid Interface Sci.* 2021, 590, 277−289.

(13) Shchukin, D. G.; Sukhorukov, G. B.; Price, R. R.; Lvov, Y. M. Halloysite Nanotubes as Biomimetic Nanoreactors. *Small* 2005, 1, 510−513.

(14) Massaro, M.; Lazzara, G.; Milioto, S.; Noto, R.; Riela, S. Covalently Modified Halloysite Clay Nanotubes: Synthesis, Properties, Biological and Medical Applications. *J. Mater. Chem. B* 2017, 5, 2867−2882.

(15) Liu, M.; Fakhrullin, R.; Novikov, A.; Panchal, A.; Lvov, Y. Tubule Nanoclay-Organic Heterostructures for Biomedical Applications. *Macromol. Biosci.* 2019, 19, 1800419.

(16) Shi, R.; Niu, Y.; Gong, M.; Ye, J.; Tian, W.; Zhang, L. Antimicrobial Gelatin-Based Elastomer Nanocomposite Membrane Loaded with Ciprofloxacin and Polymyxin B Sulfate in Halloysite Nanotubes for Wound Dressing. *Mater. Sci. Eng. Carbon* 2018, 87, 128−138.

(17) Monteiro, J. C.; Garcia, I. M.; Leitune, V. C. B.; Visioli, F.; de Souza Balbinot, G.; Samuel, S. M. W.; Makeeva, I.; Collares, F. M.; Sauro, S. Halloysite Nanotubes Loaded with Alkyl Trimethyl Ammonium Bromide as Antibacterial Agent for Root Canal Sealers. *Dent. Mater.* 2019, 35, 789−796.

(18) Garcia, I. M.; Leitune, V. C. B.; Arthur, R. A.; Nunes, J.; Visioli, F.; Giovarruscio, M.; Sauro, S.; Collares, F. M. Chemical, Mechanical and Biological Properties of an Adhesive Resin with Alkyl Trimethyl Ammonium Bromide-Loaded Halloysite Nanotubes. *J. Adhes. Dent.* 2020, 22, 399−407.

(19) Barman, M.; Mahmood, S.; Augustine, R.; Hasan, A.; Thomas, S.; Ghosal, K. Natural Halloysite Nanotubes /Chitosan Based Bio-Nanocomposite for Delivering Norfloxacin, an Anti-Microbial Agent in Sustained Release Manner. *Int. J. Biol. Macromol.* 2020, 162, 1849−1861.

(20) Khatoon, N.; Chu, M. Q.; Zhou, C. H. Nanoclay-Based Drug Delivery Systems and Their Therapeutic Potentials. *J. Mater. Chem. B* 2020, 8, 7335−7351.

(21) Sun, Y.; Davis, E. W. Facile Fabrication of Polydopamine Nanotubes for Combined Chemo-Photothermal Therapy. *J. Mater. Chem. B* 2019, 7, 6828−6839.

(22) Persano, F.; Batasheva, S.; Fakhrullina, G.; Gigli, G.; Leporatti, S.; Fakhrullin, R. Recent Advances in the Design of Inorganic and Nano-Clay Particles for the Treatment of Brain Disorders. *J. Mater. Chem. B* 2021, 9, 2756−2784.

(23) Yu, Q.; Chang, J.; Wu, C. Silicate Bioceramics: From Soft Tissue Regeneration to Tumor Therapy. *J. Mater. Chem. B* 2019, 7, 5449−5460.

(24) Koosha, M.; Raoufi, M.; Moravvej, H. One-Pot Reactive Electrospinning of Chitosan/PVA Hydrogel Nanofibers Reinforced

by Halloysite Nanotubes with Enhanced Fibroblast Cell Attachment for Skin Tissue Regeneration. *Colloids Surf., B* **2019**, *179*, 270−279.

(25) Flores-Santos, L., González, M. A., Dolores, B. M., Espinoza, R. E. Reactive Block Copolymers for the Preparation of Inorganic Tubule-Polymer Composites. WO 20080200601 A3, 2008.

(26) He, R.; Liu, M.; Shen, Y.; Liang, R.; Liu, W.; Zhou, C. Simple Fabrication of Rough Halloysite Nanotubes Coatings by Thermal Spraying for High Performance Tumor Cells Capture. *Mater. Sci. Eng. Carbon* **2018**, *85*, 170−181.

(27) Vergaro, V.; Abdullayev, E.; Lvov, Y. M.; Zeitoun, A.; Cingolani, R.; Rinaldi, R.; Leporatti, S. Cytocompatibility and Uptake of Halloysite Clay Nanotubes. *Biomacromolecules* **2010**, *11*, 820−826.

(28) Liu, M.; Zhang, Y.; Wu, C.; Xiong, S.; Zhou, C. Chitosan/Halloysite Nanotubes Bionanocomposites: Structure, Mechanical Properties and Biocompatibility. *Int. J. Biol. Macromol.* **2012**, *51*, 566−575.

(29) Lai, X.; Agarwal, M.; Lvov, Y. M.; Pachpande, C.; Varahramyan, K.; Witzmann, F. A. Proteomic Profiling of Halloysite Clay Nanotube Exposure in Intestinal Cell Co-Culture. *J. Appl. Toxicol.* **2013**, *33*, 1316.

(30) Ahmed, F. R.; Shoaib, M. H.; Azhar, M.; Um, S. H.; Yousuf, R. I.; Hashmi, S.; Dar, A. In-Vitro Assessment of Cytotoxicity of Halloysite Nanotubes against HepG2, HCT116 and Human Peripheral Blood Lymphocytes. *Colloids Surf., B* **2015**, *135*, 50−55.

(31) Wu, K.; Feng, R.; Jiao, Y.; Zhou, C. Effect of Halloysite Nanotubes on the Structure and Function of Important Multiple Blood Components. *Mater. Sci. Eng. Carbon* **2017**, *75*, 72−78.

(32) Wang, X.; Gong, J.; Gui, Z.; Hu, T.; Xu, X. Halloysite Nanotubes-Induced Al Accumulation and Oxidative Damage in Liver of Mice after 30-Day Repeated Oral Administration. *Environ. Toxicol.* **2018**, *33*, 623−630.

(33) Wang, X.; Gong, J.; Rong, R.; Gui, Z.; Hu, T.; Xu, X. Halloysite Nanotubes-Induced Al Accumulation and Fibrotic Response in Lung of Mice after 30-Day Repeated Oral Administration. *J. Agric. Food Chem.* **2018**, *66*, 2925−2933.

(34) Barfod, K. K.; Bendtsen, K. M.; Berthing, T.; Koivisto, A. J.; Poulsen, S. S.; Segal, E.; Verleysen, E.; Mast, J.; Holländer, A.; Jensen, K. A.; Hougaard, K. S.; Vogel, U. Increased Surface Area of Halloysite Nanotubes Due to Surface Modification Predicts Lung Inflammation and Acute Phase Response after Pulmonary Exposure in Mice. *Environ. Toxicol. Pharmacol.* **2020**, *73*, 103266.

(35) Sánchez-Fernández, A.; Peña-Parás, L.; Vidaltamayo, R.; Cué-Sampedro, R.; Mendoza-Martínez, A.; Zomosa-Signoret, V.; Rivas-Estilla, A.; Riojas, P. Synthesization, Characterization, and in Vitro Evaluation of Cytotoxicity of Biomaterials Based on Halloysite Nanotubes. *Mater.* **2014**, *7*, 7770−7780.

(36) Abhinayaa, R.; Jeevitha, G.; Mangalaraj, D.; Ponpandian, N.; Vidhya, K.; Angayarkanni, J. Cytotoxic Consequences of Halloysite Nanotube/Iron Oxide Nanocomposite and Iron Oxide Nanoparticles upon Interaction with Bacterial, Non-Cancerous and Cancerous Cells. *Colloids Surf., B* **2018**, *169*, 395−403.

(37) Loos, C.; Syrovets, T.; Musyanovych, A.; Mailänder, V.; Landfester, K.; Ulrich Nienhaus, G.; Simmet, T. Functionalized Polystyrene Nanoparticles as a Platform for Studying Bio-Nano Interactions. *Beilstein J. Nanotechnol.* **2014**, *5*, 2403−2412.

(38) Zazenski, R.; Ashton, W. H.; Briggs, D.; Chudkowski, M.; Kelse, J. W.; Maceachern, L.; Mccarthy, E. F.; Nordhauser, M. A.; Roddy, M. T.; Teetsel, N. M.; Wells, A. B.; Gettings, S. D. Talc: Occurrence, Characterization, and Consumer Applications. *Regul. Toxicol. Pharmacol.* **1995**, *21*, 218−229.

(39) Wang, X.; Guo, J.; Chen, T.; Nie, H.; Wang, H.; Zang, J.; Cui, X.; Jia, G. Multi-Walled Carbon Nanotubes Induce Apoptosis via Mitochondrial Pathway and Scavenger Receptor. *Toxicol. In Vitro* **2012**, *26*, 799−806.

(40) Yin, S.; Meng, Q.; Zhang, B.; Shi, B.; Shan, A.; Li, Z. Alleviation of Zearalenone Toxicity by Modified Halloysite Nanotubes in the Immune Response of Swine. *Food Addit. Contam., Part A* **2015**, *32*, 87−99.

(41) Wu, H.; Shi, Y.; Huang, C.; Zhang, Y.; Wu, J.; Shen, H.; Jia, N. Multifunctional Nanocarrier Based on Clay Nanotubes for Efficient Intracellular SiRNA Delivery and Gene Silencing. *J. Biomater. Appl.* **2014**, *28*, 1180−1189.

(42) Toledano-Magaña, Y.; Flores-Santos, L.; Montes De Oca, G.; González-Montiel, A.; Laclette, J. P.; Carrero, J. C. Effect of Clinoptilolite and Sepiolite Nanoclays on Human and Parasitic Highly Phagocytic Cells. *BioMed Res. Int.* **2015**, *2015*, 164980.

(43) Kryuchkova, M.; Danilushkina, A.; Lvov, Y.; Fakhrullin, R. Evaluation of Toxicity of Nanoclays and Graphene Oxide in vivo: a Paramecium caudatum Study. *Environ. Sci.: Nano* **2016**, *3*, 442−452.

(44) Fakhrullina, G.; Akhatova, F.; Lvov, Y.; Fakhrullin, R. Toxicity of Halloysite Clay Nanotubes in vivo: a Caenorhabditis elegans Study. *Environ. Sci.: Nano* **2015**, *2*, 54.

(45) Long, Z.; Wu, Y.-P.; Gao, H.-Y.; Zhang, J.; Ou, X.; He, R.-R.; Liu, M. In vitro and in vivo Toxicity Evaluation of Halloysite Nanotubes. *J. Mater. Chem. B* **2018**, *6*, 7204−7216.

(46) Massaro, M.; Cavallaro, G.; Colletti, C. G.; Lazzara, G.; Milioto, S.; Noto, R.; Riela, S. Chemical Modification of Halloysite Nanotubes for Controlled Loading and Release. *J. Mater. Chem. B* **2018**, *6*, 3415−3433.

(47) Khatoon, N.; Chu, M. Q.; Zhou, C. H. Nanoclay-Based Drug Delivery Systems and Their Therapeutic Potentials. *J. Mater. Chem. B* **2020**, *8*, 7335−7351.

(48) Berger, A. Science Commentary: Th1 and Th2 Responses: What Are They? *Br. Med. J.* **2000**, *321*, 424.

(49) Morimoto, Y.; Ogami, A.; Todoroki, M.; Yamamoto, M.; Murakami, M.; Hirohashi, M.; Oyabu, T.; Myojo, T.; Nishi, K.-I.; Kadoya, C.; Yamasaki, S.; Nagatomo, H.; Fujita, K.; Endoh, S.; Uchida, K.; Yamamoto, K.; Kobayashi, N.; Nakanishi, J.; Tanaka, I. Expression of Inflammation-Related Cytokines Following Intratracheal Instillation of Nickel Oxide Nanoparticles. *Nanotoxicology* **2010**, *4*, 161−176.

(50) Song, C.; Luo, L.; Lei, Z.; Li, B.; Liang, Z.; Liu, G.; Li, D.; Zhang, G.; Huang, B.; Feng, Z.-H. IL-17-Producing Alveolar Macrophages Mediate Allergic Lung Inflammation Related to Asthma. *J. Immunol.* **2008**, *181*, 6117−6124.

(51) Annas, A.; Bengtsson, C.; Törnqvist, E. Group Housing of Male CD1 Mice: Reflections from Toxicity Studies. *Lab. Anim.* **2013**, *47*, 127−129.

(52) Aalapati, S.; Ganapathy, S.; Manapuram, S.; Anumolu, G.; Prakya, B. M. Toxicity and Bio-Accumulation of Inhaled Cerium Oxide Nanoparticles in CD1 Mice. *Nanotoxicology* **2014**, *87*, 786−798.

(53) Longmire, M.; Choyke, P. L.; Kobayashi, H. Clearance Properties of Nano-Sized Particles and Molecules as Imaging Agents: Considerations and Caveats. *Nanomedicine* **2008**, *3*, 703−717.

(54) Rong, R.; Zhang, Y.; Zhang, Y.; Hu, Y.; Yang, W.; Hu, X.; Wen, L.; Zhang, Q. Inhibition of Inhaled Halloysite Nanotube Toxicity by Trehalose through Enhanced Autophagic Clearance of P62. *Nanotoxicology* **2019**, *13*, 354−368.

(55) Ingerman, L.; Jones, D. J.; Rosemond, Z. *Toxicological Profile for Aluminum*; Taylor and Francis Group, 2008.

(56) Fizir, M.; Dramou, P.; Dahiru, N. S.; Ruya, W.; Huang, T.; He, H. Halloysite Nanotubes in Analytical Sciences and in Drug Delivery: A Review. *Microchim. Acta* **2018**, *185*, 389.

(57) Takeda, K.; Suzuki, K.; Ishihara, A.; Kubo-Irie, M.; Fujimoto, R.; Tabata, M.; Oshio, S.; Nihei, Y.; Ihara, T.; Sugamata, M. Nanoparticles Transferred from Pregnant Mice to Their Offspring Can Damage the Genital and Cranial Nerve Systems. *J. Heal. Sci.* **2009**, *55*, 95−102.

(58) Yoshida, S.; Hiyoshi, K.; Ichinose, T.; Takano, H.; Oshio, S.; Sugawara, I.; Takeda, K.; Shibamoto, T. Effect of Nanoparticles on the Male Reproductive System of Mice. *Int. J. Androl.* **2009**, *32*, 337−342.

(59) Yoshida, S.; Hiyoshi, K.; Oshio, S.; Takano, H.; Takeda, K.; Ichinose, T. Effects of Fetal Exposure to Carbon Nanoparticles on Reproductive Function in Male Offspring. *Fertil. Steril.* **2010**, *93*, 1695−1699.

(60) Campagnolo, L.; Massimiani, M.; Palmieri, G.; Bernardini, R.; Sacchetti, C.; Bergamaschi, A.; Vecchione, L.; Magrini, A.; Bottini, M.; Pietroiusti, A. Biodistribution and Toxicity of Pegylated Single Wall Carbon Nanotubes in Pregnant Mice. *Part. Fibre Toxicol.* **2013**, *10*, 1.

(61) Roychoudhury, S.; Nath, S.; Massanyi, P.; Stawarz, R.; Kacaniova, M.; Kolesarova, A. Copper-Induced Changes in Reproductive Functions: In Vivo and In Vitro Effects. *Physiol. Res.* **2016**, *65*, 11−22.

(62) Turner, P. V.; Brabb, T.; Pekow, C.; Vasbinder, M. A. Administration of Substances to Laboratory Animals: Routes of Administration and Factors to Consider. *J. Am. Assoc. Lab. Anim. Sci.* **2011**, *50*, 600−613.